Second Conference on Smart Monitoring,
Assessment and Rehabilitation of Civil Structures

SMAR 2013

Post-tensioning for rehabilitation of the in-plane behavior of structural masonry walls

A. Sadeghi Marzaleh[1], B. Weber[1], K. Pfyl-Lang[2], and M. Motavalli[1]

[1] Empa, Swiss Federal Laboratories for Materials Science and Technology, Dübendorf, Switzerland
[2] Building Department Canton Zürich, Zürich, Switzerland

ABSTRACT: The seismic vulnerability of structural unreinforced masonry (URM) walls is rather high because masonry has low tensile strength. As a retrofitting method, a post-tensioning technique can be employed to enhance the in-plane behavior of the masonry walls. A series of static cyclic in-plane experiments was performed on URM walls with different geometries with and without post-tensioning. The masonry walls were built using solid clay bricks and weak mortar representing the material mainly used in construction of buildings in Switzerland at the beginning of the last century. Post-tensioning was applied by means of external prestressing bars installed on both sides of the walls. A 3D image correlation system was employed for capturing the full-field displacement of the walls. The test results show a significant increase in the shear resistance of the post-tensioned walls. However, their displacement capacity decreased to some extent depending on the geometry and the failure mode.

1 INTRODUCTION

In residential masonry buildings, the lateral load imposed by seismic actions is carried by structural masonry walls. The seismic vulnerability of these elements is rather high because masonry has low tensile strength. As a retrofitting method, a post-tensioning technique can be employed to enhance the in-plane behavior of the masonry walls. The effectiveness of this technique for new buildings in seismic areas has been proven by Laursen and Ingham (2001) for concrete masonry and by Rosenboom and Kowalsky (2004) for hollow clay brick masonry. On this basis, a project was defined at Empa aiming at assessing the applicability of the method for existing buildings as a retrofitting technique. Solid clay bricks and weak mortar were used for constructing large-scale URM walls representing the material mainly used in construction of buildings in Switzerland at the beginning of the last century. The focus of this paper is on the investigation of effects of post-tensioning on the in-plane behavior of URM walls with different aspect ratios constructed with the specified material.

2 CONSTRUCTION DETAILS

2.1 Wall specimens

Four large-scale cantilever wall specimens were tested. Since the failure mode of masonry walls is largely influenced by their aspect ratio, two different aspect ratios were considered with one wall type being fairly squat and the other one being fairly slender. The squat and slender walls were designed to experience shear and flexural failure modes, respectively. The test program of the walls is shown in Table 1. For more clarification Wall 4 is shown in Figure 1.

Table 1.Test program

Specimen	length (m)	height (m)	thickness (m)	vertical load (kN)	post-tensioning (kN)	normal stress (MPa)
Wall 1	2.85	1.9	0.12	114	0	0.33
Wall 2	2.85	1.9	0.12	114	160	0.80
Wall 3	1.58	1.9	0.12	62	0	0.33
Wall 4	1.58	1.9	0.12	62	84	0.77

2.2 Material properties

2.2.1 Masonry

The masonry used for the tests was intended to represent the masonry used for residential buildings in Switzerland at the beginning of the last century. Such masonry was characterized by solid clay bricks and a lime or lime-cement mortar with rather low compressive strength.

The bricks used were solid bricks with a guaranteed compressive strength of 28 MPa. These bricks are produced nowadays for façades and not for structural walls. Bricks with a lower compressive strength are not produced anymore in Switzerland. The bricks had a nominal size of 250 mm x 120 mm x 60 mm. The compressive strength was determined according to the standard EN 772-1 (2000). The bricks showed an average compressive strength of 39.5 MPa with a standard deviation of 12.5 MPa.

A weak lime-cement mortar with a proportion of cement:lime:sand of 1:2:9 was chosen. Compressive strength and flexural tensile strength were determined according to EN 1015-11 (1999). The compression tests resulted in a mean compressive strength of 2.5 MPa with a standard deviation of 0.7 MPa.

2.2.2 Prestressing bars

SpannStahl M13x1.5 high-strength threaded bars were used to apply post-tensioning to Walls 2 and 4. The diameter of these bars is 12 mm and their yield strength and modulus of elasticity are 1335 MPa and 210 GPa respectively.

2.3 Testing details

2.3.1 Test set-up

The test set-up for the slender masonry walls is shown in Figure 1. The principal components are specified in the figure. For the squat walls, the same components were used except that longer components were constructed for the foundation and the loading beam.

The walls were directly constructed on the foundation which had been placed at the final position on the strong floor. For the uppermost bed joint between the wall and the loading beam a cement mortar with a higher strength and a layer of a special adhesive (SikaDur 30) were used to prevent sliding between the specimen and the loading beam.

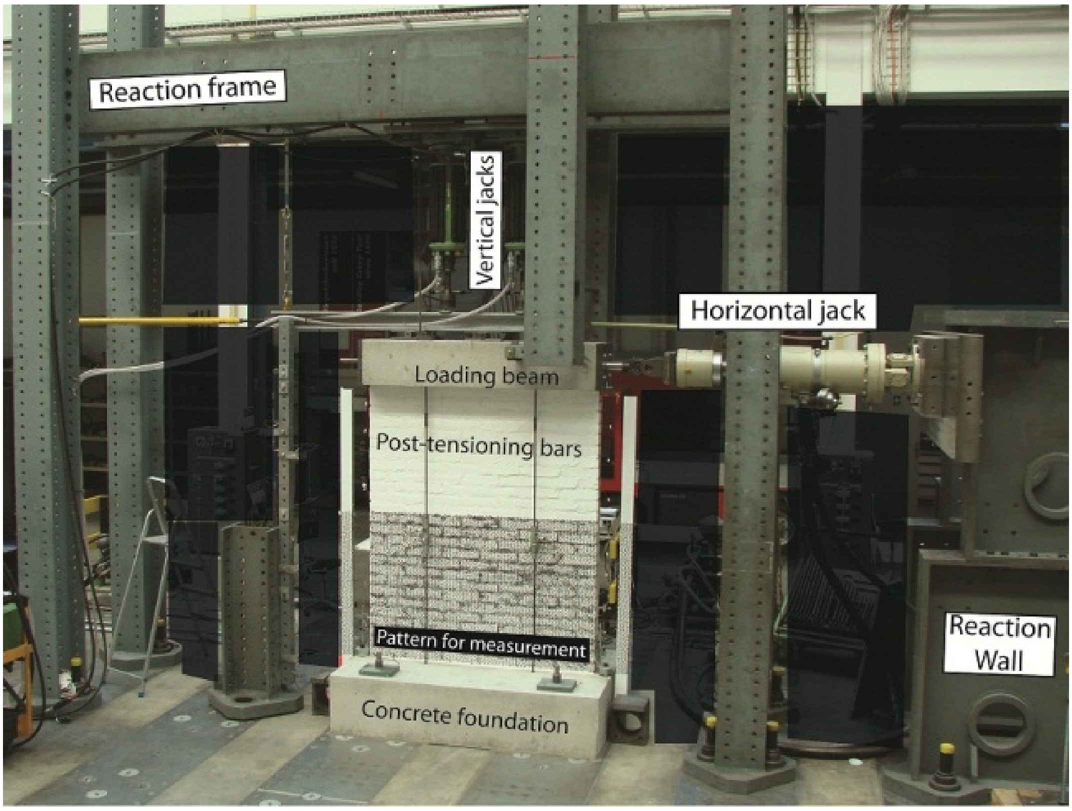

Figure 1. Test set-up of the slender walls.

Post-tensioning of Wall 2 and Wall 4 was applied by means of external prestressing bars on both sides of the walls symmetrically. For the squat wall (Wall 2), eight prestressing bars, four on each side, were positioned along the length of the wall with a spacing of 700 mm between the bars. For the slender wall (Wall 4) only two prestressing bars on each side were used with a spacing of 750 mm (cf. Figure 1). After the construction of the walls, the prestressing bars passing through the holes in the loading beam were anchored in the embedded plates of the foundation at one end and on the top of the loading beam at the other one.

Two vertical jacks were used to apply the axial force to the walls representing the dead and live loads in a building. The loads provided by the vertical jacks were transferred to the loading beam using a stiff steel beam and three roller supports placed symmetrically beneath the steel beam. The servo-hydraulic jack, shown in Figure 1, was used to apply the horizontal cyclic in-plane force to the walls.

2.3.2 Instrumentation

Figure 2 shows schematically a typical wall instrumentation. The horizontal force was measured by a load cell positioned in line with the horizontal jack. 14 displacement transducers were installed on each wall. The forces in the post-tensioning bars were measured by means of the four load cells K1 to K4 which were installed in series with them as indicated in Figure 2 for Wall 4.

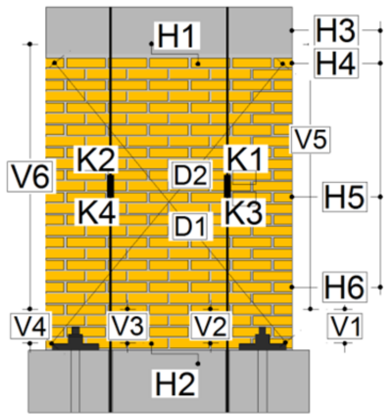

Figure 2. Typical instrumentation (The load cells K1 and K3 were installed on the other side of the wall).

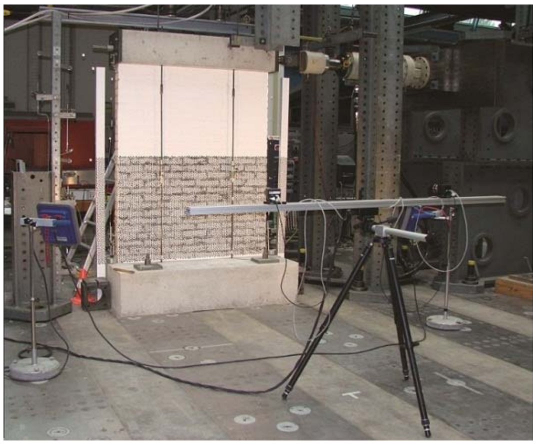

Figure 3. 3D image correlation system installation of Wall 4.

2.3.3 3D image correlation system

In addition to the conventional measurements with displacement transducers, optical measurements were carried out with a 3D image correlation system using the commercial product ARAMIS (2008). The installation of the image correlation system for Wall 4 is shown in Figure 3. This system encompasses two 4-mega pixel cameras with focal length of 20 mm. A random pattern is painted on the wall that allows comparing the two stereo photos of a specimen in a deformed state with those of the initial state. The image correlation system compares so-called facets of 15 x 15 pixels. With this setup, the displacement resolution is around 0.1 to 0.01 pixels. For the squat walls, the side length of the measuring window of 4 m is mapped into 2000 pixels. This corresponds to 2 mm/pixel and results in a resolution of 0.2 to 0.02 mm. For the slender walls, a smaller measuring window was chosen, covering only the lower half of the wall and resulting in a resolution of 0.1 to 0.01 mm.

2.3.4 Testing procedure

Before running the tests, all displacement transducers were set to zero and the 3D image correlation system was calibrated. Then, the vertical loads were imposed by the vertical jacks. The total vertical load was kept constant over the whole duration of the test without imposing a moment. After the application of the vertical loads, the post-tensioning was applied if applicable (Walls 2 and 4) and the forces at the load cells were recorded.

The horizontal loading history was then applied to the walls in a way similar to the one defined for the European Project ESECMaSE (Magenes et al, 2008). However, instead of imposing the first load step force-controlled the complete loading history was imposed displacement-controlled. At each load step, three cycles were performed before the target displacement was increased.

In every maximum and minimum displacement, the horizontal jack was stopped in order to report the new cracks and do the optical measurements.

3 TEST RESULTS

3.1 Damage pattern and failure mode

Figure 4 shows the final state of the walls. All walls showed initially a rocking behavior with a single flexural crack opening at the tension side and, with increasing horizontal displacements, additional nearly vertical cracks in the compression zones.

For both squat walls, the first visible cracks formed in the bed joints during the load step with a target drift of the horizontal jack of 0.15%. These cracks did not necessarily form in the bottom bed joint but two or three layers higher up and then stepped down to the bottom bed joint towards the center of the wall.

For the slender wall without post-tensioning (Wall 3), the first crack was observed in the 8th bed joint above the foundation slab already at 0.04% drift of the horizontal jack. However, once the flexural cracks formed in the bottom mortar bed joint, the first crack remained closed. For the slender wall with post-tensioning (Wall 4), the flexural cracks in the bottom mortar bed joint started to form at 0.075% drift of the horizontal jack.

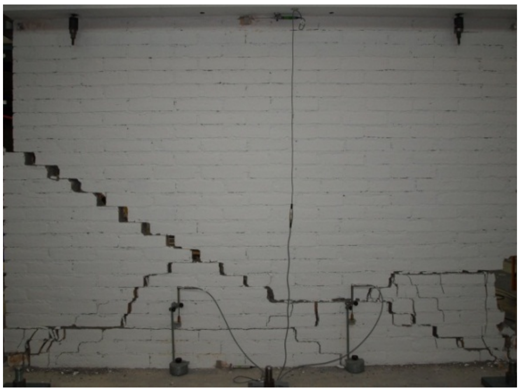

(a)

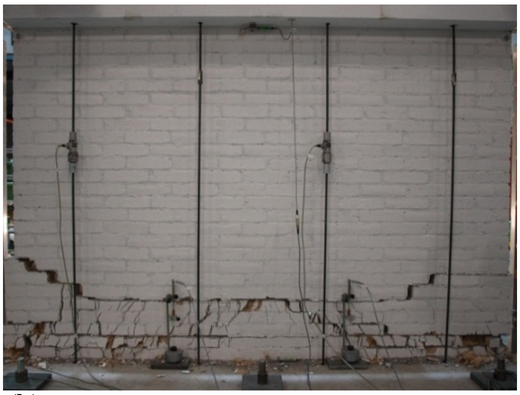

(b)

(c)

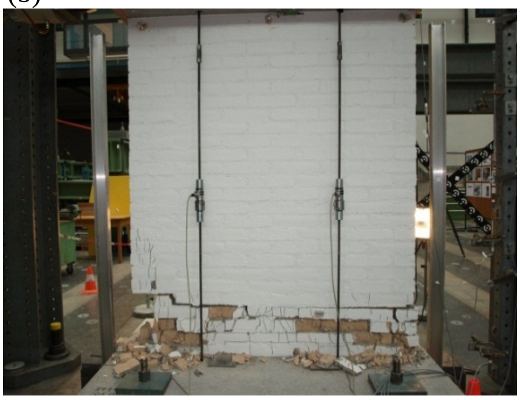

(d)

Figure 4. The final state of (a) Wall 1, (b) Wall 2, (c) Wall 3 and (d) Wall4.

After the initial rocking behavior, a diagonal stepped crack opened in the squat wall without post-tensioning (Wall 1), at a target displacement of the horizontal jack of 0.6%. This changed the behavior of the wall from rocking to sliding. At the same time large vertical cracks formed in the compression zones and spalling of the bricks in the most compressed corners occurred. In contrast, the slender wall without post-tensioning (Wall 3) did not change to a sliding mode and showed an almost pure rocking behavior with a flexural crack in the bottom mortar bed joint and localized damages in the compression zones. In fact, the test on Wall 3 was stopped before the ultimate condition of the wall was reached because of the limits of the test set-up (fixation of the steel beam and displacement capacity of the horizontal jack). At the end of the test, the maximum horizontal drift was over 4.0% without significant loss of the horizontal resistance.

The two post-tensioned walls, the squat Wall 2 and the slender Wall 4, showed both a predominant rocking behavior. However, in both cases the damaged zones were much more extended with vertical cracks over the whole bottom part of the walls. In fact, once the damaged zones extended to the center of the walls, new tensile flexural cracks formed above the damaged zones leading to a modified rocking behavior about them. In addition, the rocking movement of Wall 2 was accompanied by an increasing sliding movement along the new tensile flexural cracks in both directions. This led to the compression zones being pushed outwards producing an increasing offset between the bottom layers below the newly formed tensile flexural cracks and the layers above them.

3.2 *Horizontal force-displacement relationship*

Figure 5 depicts the horizontal force-drift of the walls. In this figure, the dash line shows the last load step based on the displacement protocol introduced to the horizontal jack.

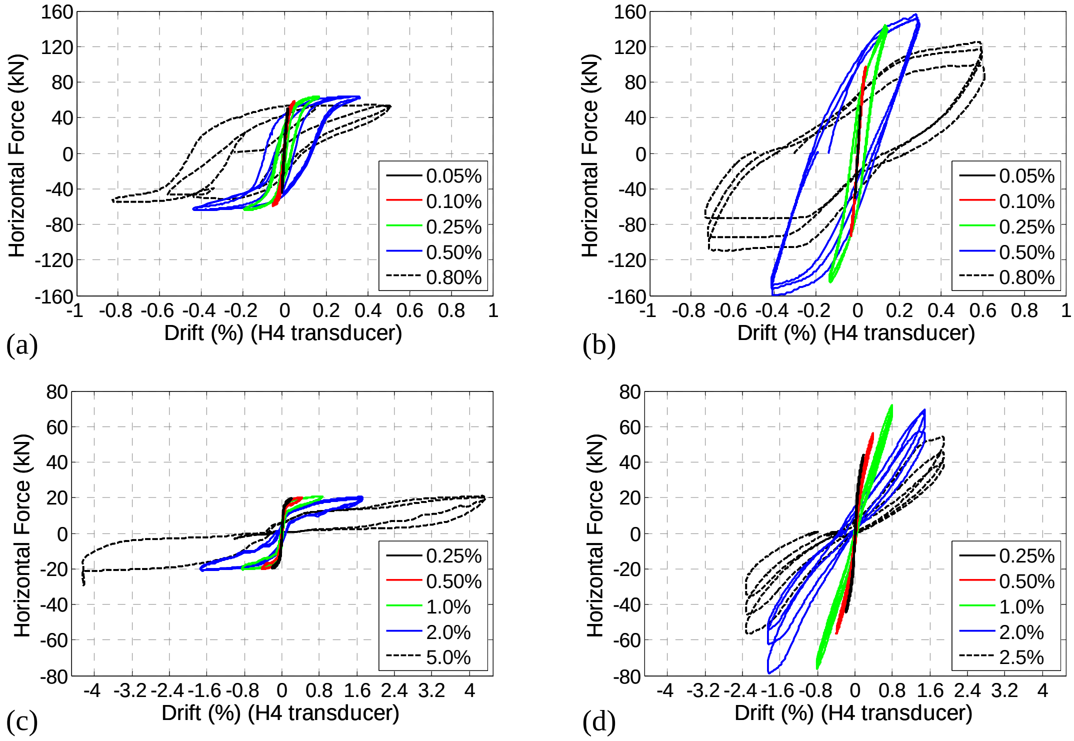

Figure 5. Horizontal force versus drift of (a) Wall 1, (b) Wall 2, (c) Wall 3 and (d) Wall 4 for different drifts of the horizontal jack (H3 transducer).

The initial rocking behavior of Wall 1 was well reflected by the horizontal force-displacement curves with the wall returning very close to the origin after each cycle. Simultaneously the wall was sliding on the tensile cracks, which opened the hysteretic curve gradually. By forming the diagonal stair stepped crack, the behavior changed from rocking to sliding over this crack and the hysteretic curve opened significantly leading to large residual displacements.

Also Wall 2 started initially with rocking and sliding over the tensile flexural cracks. The increasing sliding movement is well reflected by the growing opening of the hysteretic curves and, hence, the increasing residual displacements in the unloaded state. After several steps, due to high compressive stresses, toe regions crushed that resulted finally in the degradation of stiffness and strength.

Wall 3, the slender wall without post-tensioning, showed an almost pure rocking behavior up to the very last load steps when a concentrated toe crushing occurred. The residual displacements in the unloaded state before toe-crushing were less than 1 mm. Only during the final load steps the hysteretic curves opened up, however, the residual displacements remained small, i.e. the wall returned almost to its original position at the end of the test.

Also Wall 4, the slender wall with post-tensioning, showed a pronounced rocking behavior. However, whereas Wall 3 showed a flag type behavior, the behavior of Wall 4 showed no distinct plateau. The behavior at each load step was more "linear" and the opening of the hysteretic curves remained limited. Crushing of the both bottom corners led to a decrease in the stiffness and strength of the wall.

4 DISCUSSION

4.1 Effect of post-tensioning on the shear resistance

As can be seen in Figure 5, post-tensioning enhances the shear resistance of both squat and slender walls. Two different mechanisms can be considered responsible in the two cases. The first mechanism is more effective in the squat wall where the applied post-tensioning increases the normal stress on the sliding parts. Hence, the friction between them becomes greater and the diagonal stepped cracking is prevented. As a result, the failure mode changes to toe crushing and the shear resistance increases. The other mechanism occurs notably in the post-tensioned slender wall where the rocking mode generates extra axial force in the post-tensioning bars due to vertical displacement of the loading beam. The generated axial force in the bars, especially those located further from the rotation center of rocking, provides a moment that resists the imposed horizontal force. The more horizontal displacement is introduced to the wall, the larger resisting moments the post-tensioning bars generate.

Shear resistance of post-tensioned walls decreases when new full-length tensile cracks occur and the bottom corners crush. Due to the loss of strength at the corners the rotation center moves toward the mid-length of the wall. As a result, the elongation of post-tensioning bars decreases and therefore the resisting moment becomes smaller. Figure 6 shows the optically measured vertical displacement of the post-tensioned walls at the final load step. Only the bottom half of the slender wall was measured optically (Figure 3). It can be seen in the figure that in the slender wall, the vertical displacement is much larger, which shows that the latter mechanism is more pronounced.

4.2 Effect of post-tensioning on the in-plane displacement

Concerning the deformation capacity which is of crucial importance for the seismic behavior of the walls, the post-tensioned squat Wall 2 only showed a minor reduction with respect to the reference Wall 1 without post-tensioning. For the slender walls the deformation capacity was however reduced due to the post-tensioning, but the final drift capacity of the post-tensioned wall was still more than 1.5% which is superior to the corresponding value of 0.8% given in FEMA-356 for generalized force-deformation relation of masonry elements in case of analyzing structures using the nonlinear static procedure (NSP).

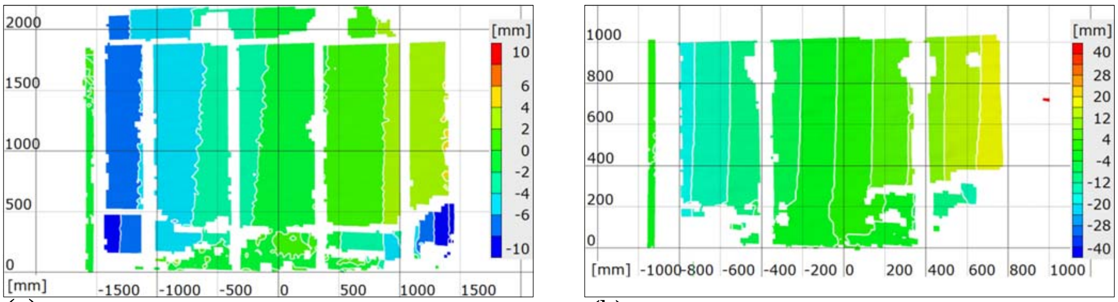

(a) (b)

Figure 6. Contour of vertical displacement at the last loading step for (a) Wall 2 and (b) Wall 4.

5 CONCLUSIONS AND FUTURE DEVELOPMENTS

The main objective of this study was to investigate the effect of post-tensioning on unreinforced masonry walls with weak mortar and different aspect ratios.

The tests have confirmed that the post-tensioning increases the shear resistance of masonry walls. Even though the post-tensioning applied to the squat and slender walls was rather similar, two different mechanisms were dominant in each of them. The first mechanism prevents a diagonal stepped cracking by increasing the friction between sliding parts in the squat wall and the second increases the resisting moment produced by elongation of bars in the slender one.

The displacement capacity was decreased in both cases. However, a major decrease was only observed in the slender wall, where the wall shows a large increase in shear resistance due to post-tensioning and the displacement capacity is still about double of the conservative value of codes.

It is evident that this method of retrofitting is not suitable for the URM walls that already have high stresses because of the inherent property of the method in increasing their axial stress. The investigation of effects of post-tensioning on URM walls with higher axial stresses will be pursued in the future.

6 REFERENCES

Laursen, PT, Ingham, JM, and Kahn, LF. 2001. Structural testing of single-storey post-tensioned concrete masonry walls. *The Masonry Society Journal*, 19(1): 69-82.

Rosenboom, OA, and Kowalsky, MJ. 2004. Reversed in-plane cyclic behavior of posttensioned clay brick masonry walls. *Journal of Structural Engineering*, 130(5): 787-798.

European Standard. 2000. Methods of tests for masonry units-Part 1: Determination of compressive strength. EN 772-1. Brussels, Belgium.

European Standard. 1999. Methods of test for mortar for masonry-Part 11: Determination of flexural and compressive strength of hardened mortar. EN 1015-11. Brussels, Belgium.

ARAMIS. 2008. v. 6.1 User's Manual. GOM mbH. Braunschweig, Germany.

Magenes, G, Morandi, P, Penna, A. 2008. Experimental in-plane cyclic response of masonry walls with clay units. *Proceedings of the 14th World Conference on Earthquake Engineering*, October 12-17 2008, Beijing, China, Paper ID: 12-03-0095.

Building Seismic Safety Council (BSSC). 2000. Prestandard and commentary for the seismic rehabilitation of buildings. Rep. FEMA-356. Washington, D.C.